THE JOURNAL OF BIOLOGICAL CHEMISTRY VOL. 288, NO. 37, pp. 26583–26593, September 13, 2013

Development of a Human IgG4 Bispecific Antibody for Dual Targeting of Interleukin-4 (IL-4) and Interleukin-13 (IL-13) Cytokines*

Received for publication, April 30, 2013, and in revised form, July 16, 2013 Published, JBC Papers in Press, July 23, 2013, DOI 10.1074/jbc.M113.480483

Christoph Spiess[‡1], Jack Bevers III[‡], Janet Jackman[§], Nancy Chiang[‡], Gerald Nakamura[‡], Michael Dillon[‡], Hongbin Liu[¶], Patricia Molina[¶], J. Michael Elliott[‖], Whitney Shatz[‖], Justin M. Scheer[‖], Glen Giese[**], Josefine Persson[**], Yin Zhang[‡], Mark S. Dennis[‡], James Giulianotti[‡‡], Prateek Gupta[‡‡2], Dorothea Reilly[‡‡], Enzo Palma[§§], Jianyong Wang[¶¶], Eric Stefanich[§§], Heleen Scheerens[‖‖], Germaine Fuh[‡3], and Lawren C. Wu[§4]

From the Departments of [‡]Antibody Engineering, [§]Immunology, [¶]Protein Analytical Chemistry, [‖]Protein Chemistry, [**]Purification Development, [‡‡]Early Stage Cell Culture, [§§]Preclinical and Translational Pharmacokinetics and Pharmacodynamics, [¶¶]Biochemical and Cellular Pharmacology, and [‖‖]Pharmacodynamic Biomarkers, Genentech Research and Early Development, South San Francisco, California 94080

Background: Dual neutralization of IL-4 and IL-13 is a promising therapeutic approach for asthma and allergy.
Results: Knobs-into-holes IgG1 and IgG4 bispecific antibodies targeting both cytokines were developed.
Conclusion: Bispecific antibodies of both isotypes have comparable *in vitro* potencies, *in vivo* pharmacokinetics, and lung partitioning.
Significance: Further extension of knobs-into-holes technology to human IgG4 isotype as reported here provides greater options for therapeutics.

Human bispecific antibodies have great potential for the treatment of human diseases. Although human IgG1 bispecific antibodies have been generated, few attempts have been reported in the scientific literature that extend bispecific antibodies to other human antibody isotypes. In this paper, we report our work expanding the knobs-into-holes bispecific antibody technology to the human IgG4 isotype. We apply this approach to generate a bispecific antibody that targets IL-4 and IL-13, two cytokines that play roles in type 2 inflammation. We show that IgG4 bispecific antibodies can be generated in large quantities with equivalent efficiency and quality and have comparable pharmacokinetic properties and lung partitioning, compared with the IgG1 isotype. This work broadens the range of published therapeutic bispecific antibodies with natural surface architecture and provides additional options for the generation of bispecific antibodies with differing effector functions through the use of different antibody isotypes.

Monoclonal antibodies have led to the generation of widely successful therapeutics. However, these treatments often do not completely ameliorate disease. Because monoclonal antibodies target only a single antigen, whereas multiple pathogenic mediators are often dysregulated in human diseases, bispecific antibodies that can simultaneously target two different antigens may have the potential to improve therapeutic outcomes.

A vast number of bispecific antibody and antibody-like formats have been developed (1), but few have progressed as therapeutic agents into human clinical trials. Twelve bispecific molecules are currently being evaluated in clinical studies (2), and one, catumaxumab (3), has been approved in the European Union. Despite these advances, these bispecific molecule formats still have limitations that restrict their general clinical utility. For example, the small size of some of these molecules leads to short pharmacokinetic properties that are extended by frequent dosing intervals, continuous delivery, or fusion to albumin binding domains (4). In addition, most of these bispecific formats contain non-natural or non-human sequences that serve as linkers, binding sites, or heterodimerization domains. These sequences can lead to poor stability, aggregation, and large scale manufacturing challenges. Furthermore, they increase the risk of immunogenicity, thereby precluding their use in settings that require long term drug administration.

The development of full-length bispecific antibodies with natural human antibody architectures could overcome many of the limitations of other bispecific molecule formats. Human antibodies have a long serum half-life that is due to the binding of their Fc regions to the neonatal receptor, FcRn. A variety of solutions have been developed to drive efficient heterodimerization of full-length human antibody heavy chains (5–8). However, there have been few solutions to prevent mispairing of light chains without the use of linkers (9, 10).

One way to promote heterodimerization of antibody heavy chains is by introducing knobs-into-holes mutations in the C_H3

* All authors are or have been employed by Genentech, which develops and markets drugs for profit.

[1] To whom correspondence may be addressed: Department of Antibody Engineering, Genentech Research and Early Development, 1 DNA Way, South San Francisco, CA, 94080. Tel.: 650-467-1851; Fax: 650-467-8318; E-mail: christsp@gene.com.
[2] Present address: Total New Energies USA, 5858 Horton St., Emeryville, CA 94608.
[3] To whom correspondence may be addressed: Dept. of Antibody Engineering, Genentech Research and Early Development, 1 DNA Way, South San Francisco, CA 94080. Tel.: 650-225-2308; Fax: 650-467-8318; E-mail: gml@gene.com.
[4] To whom correspondence may be addressed: Dept. of Immunology, Genentech Research and Early Development, 1 DNA Way, South San Francisco, CA, 94080. Tel.: 650-225-1548; Fax: 650-467-8318; E-mail: lawren@gene.com.

dimer interface. This technology has been used previously to generate bispecific antibodies of IgG1 subclass with a common light chain (11, 12) and has subsequently been extended to bispecific antibodies with two different light chains through the use of linker sequences (13) or domain swaps (14). Recently, we developed a method to express heavy-light half-antibodies (hemimers) that are subsequently combined to form an intact bispecific immunoglobulin in order to generate bispecific antibodies with two different light chains without the use of non-natural linkers or domain swaps (15, 16). To date, the knobs-into-holes technology has not been reported in the scientific literature for other human antibody isotypes beyond IgG1.

Interleukin-4 (IL-4) and interleukin-13 (IL-13) are two cytokines that are associated with type 2 inflammation (17–21). IL-4 binds to two receptors, one a heterodimer of IL-4 receptor α (IL-4Rα)[5] and the common γ chain (γ_c) and the other a heterodimer of IL-4Rα and IL-13 receptor α1 (IL-13Rα1). The latter receptor, IL-4Rα·IL-13Rα1, is a shared receptor with IL-13, which also uniquely binds a single chain receptor consisting of IL-13 receptor α2 (IL-13Rα2).

A number of studies have implicated IL-4, IL-13, and their receptors in the pathogenesis of asthma and allergy (22–26). Polymorphisms of the IL-4, IL-13, and IL-4Rα genes are associated with asthma and allergy, including features such as IgE levels, prevalence of atopy, and severity of asthma disease. In addition, expression of IL-4, IL-13, and their receptors are increased in asthma and other allergic diseases. Moreover, neutralization or deficiency of IL-4, IL-13, and their receptors ameliorates disease in preclinical models of asthma.

Recently, several studies have shown clinical activity of monoclonal antibodies against IL-13 in the treatment of asthma (27–31). Of these, lebrikizumab, a humanized IgG4 antibody that neutralizes IL-13 activity, improved lung function in moderate-to-severe asthmatics, particularly in the subgroup with high serum periostin, a systemic biomarker of IL-13 (27). Given the distinct and overlapping roles for IL-4 and IL-13 in type 2 inflammation, dual neutralization of IL-4 and IL-13 may provide improved efficacy over single neutralization of IL-13 for the treatment of asthma.

Here we report the development of bispecific antibodies that target both IL-4 and IL-13. In order to match the bispecific antibody isotype to that of lebrikizumab, we used knobs-into-holes technology to create human IgG4 bispecifics and showed that such IgG4 bispecific antibodies can be generated with equivalent efficiency and quality and have activities comparable with those of IgG1 bispecific antibodies.

EXPERIMENTAL PROCEDURES

Generation of Anti-IL-4 Hybridoma—A panel of antibodies that selectively bind human interleukin-4 (IL-4) were generated using commercially available human IL-4 (R&D Systems, Minneapolis, MN). Each hind footpad of five BALB/c mice was injected with 0.5 μg of IL-4 resuspended in a 25-μl total volume of monophosphoryl-lipid A and trehalose dicorynomycolate (MPL^{TM} + TDM)-based adjuvant (Corixa, Hamilton, Canada) in phosphate-buffered saline (PBS) at 3–4-day intervals. Serum samples were taken after seven boosts and titers determined by an enzyme-linked immunosorbant assay (ELISA) to identify mice with a positive immune response to IL-4. Animals were boosted twice more via footpad (0.5 μg in 25 μl/footpad), intraperitoneal cavity (2 μg in 100 μl), and intravenous (1 μg in 50 μl) routes using adjuvant in PBS. Three days after the final boost, animals that showed positive serum titers by ELISA were sacrificed, and a single cell suspension of splenocytes was fused with the mouse myeloma cell line P3X63Ag.U.1 (American Type Culture Collection, Manassas, VA) using electrofusion (Cyto Pulse Sciences, Inc., Glen Burnie, MD). Fused hybridoma cells were selected from unfused splenic, popliteal node or myeloma cells using hypoxanthin-aminopterin-thymidine selection in Medium D from the ClonaCell® hybridoma selection kit (StemCell Technologies, Inc., Vancouver, Canada). Hybridoma cells were cultured in Medium E from the ClonaCell® hybridoma selection kit, and cell culture supernatants were used for further characterization and screening. To screen the 1921 hybridoma cell lines generated, an ELISA was performed generally as described earlier (32).

Humanization of 19C11—The hypervariable regions from mu19C11 were grafted into the human VL κ I and VH subgroup III consensus frameworks to generate a complementarity-determining region graft (19C11 graft) by Kunkel mutagenesis using separate oligonucleotides. Select murine vernier framework positions that might be important were individually added to the 19C11 graft to evaluate their ability to restore the affinity and function to that of mu19C11. Only two positions in VH, R71L and L78A, were required to improve binding.

Surface Plasmon Resonance BIAcore Affinity Measurement—The binding kinetics of the anti-IL-4, anti-IL-13, or anti-IL-4/IL-13 bispecific antibodies were measured using surface plasmon resonance on a Biacore 3000 instrument (GE Healthcare). Anti-human Fc (GE Healthcare) was immobilized on a CM5 sensor chip via amine-based coupling using the manufacturer-provided protocol. Antibody was captured at a level of 1200 resonance units. Bispecific binding was measured to human IL-4, cynomolgus IL-4, human IL-13, human IL-13 R130Q, and cynomolgus IL-13 at concentrations of 0, 3.13, 6.25, 12.50, 25.0, and 50.0 nM. Sensograms for binding of cytokine were recorded using an injection time of 2 min with a flow rate of 30 μl/min at a temperature of 25 °C and with a running buffer of 10 mM HEPES, pH 7.4, 150 mM NaCl, and 0.005% Tween 20. After injection, disassociation of the cytokine from the antibody was monitored for 1000 s in running buffer. The surface was regenerated between binding cycles with a 60-μl injection of 3 M magnesium chloride. After subtraction of a blank that contained running buffer only, sensograms observed for cytokine binding to anti-IL-4/anti-IL-13 bispecific antibody were analyzed using a 1:1 Langmuir binding model with software supplied by the manufacturer to calculate the kinetics and binding constants.

Plasmid Construction and Expression of Antibodies—Antibodies were cloned into expression vectors described previously (33). The STII signal sequence with a translation initia-

[5] The abbreviations used are: IL-4Rα, IL-4 receptor α; IL-13Rα1 and IL-13Rα2, IL-13 receptor α1 and α2, respectively; CE, capillary electrophoresis; PK, pharmacokinetic; BAL, bronchoalveolar lavage; ELF, epithelial lining fluid; BisTris, 2-[bis(2-hydroxyethyl)amino]-2-(hydroxymethyl)propane-1,3-diol.

tion strength of 1 for both the heavy chain and light chain preceded the sequence coding for the mature antibody. For protein expression, an overnight culture in a suitable W3110 derivative (34) was grown at 30 °C in LB (100 μg/ml carbenicillin), diluted 1:100 into CRAP medium (100 μg/ml carbenicillin), and grown for 24 h at 30 °C. For larger preparations, the cultures were grown in 10-liter fermentors as described previously (33).

For SDS-PAGE analysis under non-reducing conditions, 200 μl of overnight culture was harvested and resuspended in 100 μl of NR lysis buffer (88 μl of PopCulture reagent (Novagen), 10 μl of 100 mM iodoacetamide, 2 μl of lysonase reagent (EMD Biosciences)). After incubation for 10 min at room temperature, samples were spun for 2 min at 9300 relative centrifugal force, and 50 μl of supernatant was transferred into a fresh tube and mixed with the same volume of 2× SDS sample buffer (Invitrogen). Before loading 10 μl of the sample on NuPAGE 4–12% BisTris/MES gels (Invitrogen), samples were heated for 5 min at 95 °C and spun for 1 min at 16,000 relative centrifugal force. Gels were transferred by iBlot (Invitrogen) onto nitrocellulose membrane, immunoblotted with IRDye800CW-conjugated anti-human IgG F(c) antibody (Rockland), and imaged with a LI-COR Odyssey Imager.

For total reduced cell samples, the cell pellet was resuspended in R-lysis buffer (10 μl of 1 M dithiothreitol (DTT), 88 μl of PopCulture reagent (Novagen), 2 μl of lysonase) and incubated for 10 min at room temperature before samples were mixed with 2× SDS sample buffer. Western blots were imaged as described before with the exception that IRDye800CW-conjugated anti-human antibody (Rockland) was used for immunodetection.

Purification and Assembly of Bispecific Antibodies—*Escherichia coli* whole cell broth was homogenized using a Niro-Soavi homogenizer from GEA (Bedford, NH). The resulting homogenate was then extracted by the addition of polyethyleneimine flocculent to a final concentration of 0.4%, diluted with purified water, and mixed for 16 h at room temperature. The extract was cleared by centrifugation followed by filtration using a 0.2-μm sterile filter cooled to 15 °C and loaded on a pre-equilibrated (25 mM Tris, 25 mM NaCl 5 mM EDTA, pH 7.1) Protein A column. The column was washed with equilibration buffer and 0.4 M potassium phosphate, pH 7.0, and finally eluted with 100 mM acetic acid, pH 2.9. The Protein A pools were then combined in an assembly reaction.

The separate half-antibody Protein A pools were conditioned with 0.2 M arginine, pH-adjusted using 1.5 M Tris base to pH 8.0, and combined. L-Reduced glutathione (GSH) was added in a 200-fold molar excess over bispecific antibody, and pools were incubated at 20 °C for 48 h. After incubation, the assembled bispecific antibody was purified by an anion exchange chromatography step and a cation exchange chromatography step. The cation exchange eluate was concentrated and buffer-exchanged into final formulation buffer.

Analytical Characterization of Antibodies by Intact and Reduced Mass Spectrometric Analysis—Reduced and intact masses of bispecific antibodies were obtained by LC/MS analysis using an Agilent 6210 electrospray ionization-TOF mass spectrometer coupled with a nano-Chip-LC system. The bispecific samples, with and without prior tris(2-carboxyethyl)phosphine) reduction, at about 5 ng of antibodies per injection, were desalted by RP-HPLC for direct online MS analysis. The resulting spectra for both reduced and non-reduced samples exhibited a distribution of multiply charged protein ions, and the spectra were deconvoluted to zero charge state using the MassHunter workstation software/Qualitative Analysis B.03.01 (Agilent Technologies Inc.).

Analytical Size Exclusion Chromatography—Size variants were separated using a TosoHaas TSK G3000SW$_{XL}$ column (7.8 × 300 mm) eluted isocratically with a mobile phase consisting of 0.2 M potassium phosphate and 0.25 M potassium chloride (pH 6.2). The separation was conducted at room temperature with a flow rate of 0.5 ml/min. The column effluent was monitored at 280 nm. Relative percentage of peak areas for high molecular weight species, main peak, and low molecular weight species was determined by using the Chromeleon Software version 6.80 SR11 from Dionex Corp.

Capillary Electrophoresis-Sodium Dodecyl Sulfate Analysis (CE-SDS)—The bispecific samples were first diluted with citrate-phosphate buffer, pH 6.6, and treated with SDS and *N*-ethylmaleimide at 70 °C for 3 min. Upon cooling, samples were labeled at 50 °C for 10 min with 3-(2-furoyl)quinoline-2-carboxaldehyde) in the presence of excess potassium cyanide. The labeling reaction was quenched by buffer exchange and then treated with 1% SDS. Non-reduced samples were heated at 70 °C for 5 min. Reduced samples were treated with 50 mM DTT at 70 °C for 10 min.

Both non-reduced and reduced samples were analyzed by CE-SDS using a Beckman PA 800 CE system with a 50-μm diameter uncoated fused silica capillary. Samples were injected electrokinetically (40 s at 5 kV), and separation was performed at a constant voltage of 15 kV in reversed polarity for 35 min. Capillary temperature was maintained at 40 °C. The migration of labeled components was monitored by LIF detection; the excitation was at 488 nm, and the emission was monitored at 600 nm.

Cell Culture (TF-1)—Human TF-1 (erythroleukemic cells, R&D Systems) were cultured in a humidified incubator at 37 °C with 5% CO_2 in growth medium containing RPMI 1640 (Genentech Media Preparation Facility, South San Francisco, CA), 10% heat-inactivated fetal bovine serum (FBS) (catalogue no. SH30071.03, HyClone Laboratories, Inc. (Logan, UT)), 1× penicillin/streptomycin/glutamine (Catalogue number 10378-016, Invitrogen) and 2 ng/ml rhGM-CSF (catalogue no. 215-GM, R&D Systems). Assay medium was growth medium without 2 ng/ml rhGM-CSF. Cytokines were added to the assay medium as specified, at the following final concentrations: 0.2 ng/ml human IL-4 (catalogue no. 204-IL, R&D Systems), 10 ng/ml human IL-13 (PUR18969, Genentech, South San Francisco, CA), and 10 ng/ml human IL-13 R130Q (PUR18970, Genentech).

TF-1 Cell Proliferation Assay—Antibodies were serially diluted 3.3-fold in 50 μl of assay medium containing cytokines in a 96-well tissue culture plate (catalogue no. 353072, Falcon BD, Franklin Lakes, NJ). Plates were incubated for 30 min at 37 °C. TF-1 cells were washed twice in assay medium and resuspended at a final volume of 2.5×10^5 cells/ml. 50 μl of cells were

added to each well for a total volume of 100 μl. Plates were incubated for 4 days in a humidified incubator at 37 °C with 5% CO_2, before the addition of 1 μCi of [^{3}H]thymidine/well. After an additional 4-h incubation, proliferation was measured by cell-associated [^{3}H]thymidine incorporation using a liquid scintillation counter. Results from duplicate samples are expressed as mean values with S.E.

Data Analysis (TF-1)—Graphs were generated, and statistical analysis was performed using KaleidaGraph (Synergy Software, Reading, PA).

Pharmacokinetic Studies in Cynomolgus Monkeys—The pharmacokinetic (PK) studies in cynomolgus monkeys were approved by the institutional animal care and use committee. The PK study with anti-IL-4/IL-13 IgG4 was conducted at Charles River Laboratories Preclinical Services (Reno, NV). A total of 15 female cynomolgus monkeys (2.2–2.6 kg) from Charles River Laboratories stock were randomly assigned to five groups (n = 3/group). Animals in group 1 were given an intravenous and subcutaneous dose of the control vehicle. Animals in groups 2, 3, and 4 were given a single intravenous bolus dose of anti-IL-4/IL-13 IgG4 at 10, 30, and 100 mg/kg, respectively. Animals in group 5 were given a subcutaneous dose of anti-IL-4/IL-13 IgG4 at 10 mg/kg.

The PK study with anti-IL-4/IL-13 IgG1 was conducted at Shin Nippon Biomedical Laboratories USA (Everett, WA). A total of 12 female cynomolgus monkeys (2.4–3.1 kg) from Shin Nippon Biomedical Laboratories stock were randomly assigned to four groups (n = 3/group). Animals in group 1 were given an intravenous dose of the control vehicle. Animals in groups 2, 3, and 4 were given a single intravenous bolus dose of anti-IL-4/IL-13 IgG1 at 10, 30, and 60 mg/kg, respectively.

For both studies, serum samples were collected at various time points out to 4–5 weeks postdose, and concentrations of anti-IL-4/IL-13 IgG4 or anti-IL-4/IL-13 IgG1 were assessed by ELISA with a limit of quantitation of 0.078 μg/ml. Anti-therapeutic antibody levels were assessed by bridging ELISA. For PK data calculations, study day 1 was converted to PK day 0 to indicate the start of dose administration. The serum concentration data for each animal were analyzed using two-compartment analysis with WinNonlin®, version 5.2.1 (Pharsight, Mountain View, CA).

Lung Partitioning Study in Cynomolgus Monkeys—The lung partitioning study in cynomolgus monkeys was approved by the institutional animal care and use committee. This study comparing anti-IL-4/IL-13 IgG4 and anti-IL-4/IL-13 IgG1 was conducted at Charles River Laboratories Preclinical Services. The study consisted of two different sessions. In the first session, n = 24 cynomolgus monkeys (3–10 kg) from Charles River Laboratories stock received a base-line aerosol challenge with *Ascaris suum* to determine the suitability of the *A. suum* challenge to elicit appropriate airway responses in each animal. The animals were monitored for signs of distress throughout the challenge period and were not given antibodies during this session. Four weeks later, the second session was initiated, and a total of seven male cynomolgus monkeys were randomly assigned to two groups (n = 3 in IgG4 group; n = 4 in IgG1 group). These monkeys then received 10 mg/kg of either anti-IL-4/IL-13 IgG4 or anti-IL-4/IL-13 IgG1 via an intravenous bolus dose on study day 1 and study day 8. Subsequently, the animals were challenged via aerosol inhalation with *A. suum* on study day 9. At various time points up to 23 days postdose, bronchoalveolar lavage (BAL) fluid and serum samples were collected and analyzed for anti-IL-4/IL-13 IgG4 or anti-IL-4/IL-13 IgG1 concentrations by ELISA with a limit of quantitation of 0.078 μg/ml. For data calculations, study day 1 was converted to PK day 0 to indicate the start of dose administration. Urea and albumin were measured in BAL and serum to estimate epithelial lining fluid (ELF) concentrations and to correct for inflammation-induced vascular leakage, respectively.

RESULTS

Selection of the Parental Antibodies for a Bispecific Combination—To assemble an anti-IL-4/IL-13 bispecific antibody, we first identified suitable parental antibodies against each cytokine IL-4 and IL-13. The anti-IL-13 arm of the bispecific antibody was based on lebrikizumab, a previously generated and well characterized antibody, which binds soluble human IL-13 with a Biacore-derived K_D lower than the detection limit, 10 pM. Binding of lebrikizumab to IL-13 does not inhibit binding of IL-13 to IL-13Rα1 but does block the subsequent formation of the heterodimeric signaling-competent IL-4Rα·IL-13Rα1 complex (27, 35).

Monoclonal antibodies to human IL-4 were generated from BALB/c mice immunized with human IL-4. Clone 19C11 bound to human IL-4 with an affinity of 10 pM, as determined by surface plasmon resonance analysis. 19C11 blocked binding of biotinylated IL-4 to IL-4Rα and inhibited IL4-induced proliferation of TF-1 cells (Fig. 1), suggesting an epitope on IL-4 that overlaps with a region critical for binding to IL-4Rα. 19C11 was subsequently humanized by grafting the hypervariable region into a human $V_{\kappa\ 1}/VH_{III}$ consensus framework along with two mouse vernier positions at 71 and 78 in the variable heavy domain. The binding affinity, epitope, and cellular activity of 19C11 were conserved during the humanization process (data not shown).

Generation of Anti-IL-4/IL-13 Bispecific Antibody—We previously established a robust and versatile technology to generate human IgG1 bispecific antibodies with two different light chains in *E. coli* (15, 16). This technology utilized knobs-into-holes technology (5, 6) to promote heterodimerization of immunoglobulin heavy chains. To prevent light chain mispairing, each arm was cultured as a hemimer in separate *E. coli* cells. This approach was successful for generating an anti-IL-4/IL-13 IgG1 bispecific antibody by subcloning the anti-IL-4 and anti-IL-13 parental antibodies into vectors that expressed the anti-IL-4 arm as a human IgG1 hole and the anti-IL-13 arm as a human IgG1 knob. After expression, the soluble fractions were characterized by SDS-PAGE followed by anti-Fc immunostaining to analyze the formation of half-antibody species (Fig. 2). The intact bispecific antibody was assembled from two different protein A-purified half-antibody pools by redox chemistry.

Engineering Human IgG4 Knobs-into-holes Bispecific Antibodies—Lebrikizumab, the anti-IL-13 antibody that has shown clinical benefit in the treatment of moderate-to-severe uncontrolled asthma (27), is an IgG4 isotype antibody

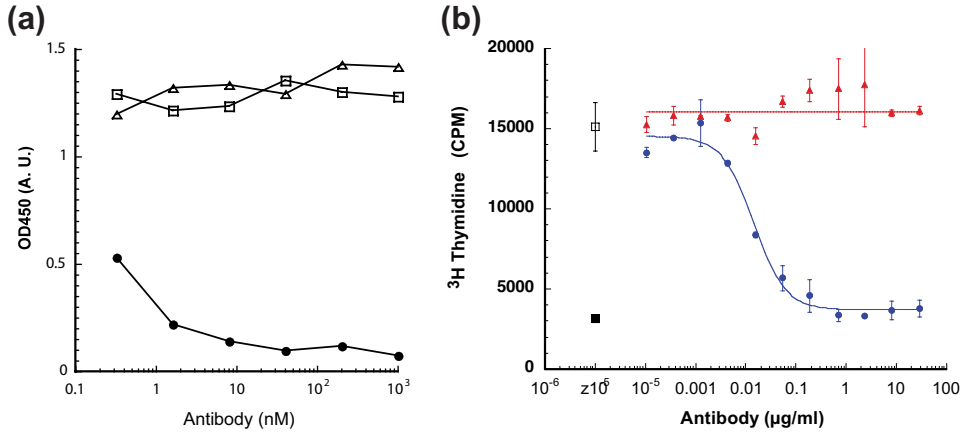

FIGURE 1. **Identification of 19C11 antibody as potent antagonist of IL-4 receptor activation.** *a*, 19C11 blocks IL-4 binding to immobilized IL-4Rα. Biotinylated IL-4 (0.17 nM) was premixed with serially diluted supernatants of IgG from clone 19C11 or a control antibody. Following incubation, the mixture was transferred to a plate containing immobilized human IL-4Rα. After washing away unbound ligand, IL-4 was detected with horseradish peroxidase-conjugated streptavidin. *Filled circles*, 19C11; *open squares*, control IgG; *open triangle*, no IgG. *b*, ability of 19C11 antibody to completely inhibit IL-4-induced proliferation of TF-1 cells. The ability to block IL-4-induced proliferation is determined by combining serial dilutions of purified 19C11 or irrelevant control antibody with IL-4 and TF-1 cells. Following a 48-h incubation, each sample received [^{3}H]thymidine, and after a 4-h incubation, incorporation of [^{3}H]thymidine was determined. *Open square*, no antibody added; *filled triangles*, negative control antibody; *filled circles*, 19C11; *filled squares*, no IL-4 added. *A.U.*, absorbance units. Error bars, S.E.

with a stabilizing S228P mutation in the hinge region. We are unaware of any reports in the scientific literature describing the expression of IgG4 antibodies in *E. coli* or the application of the knobs-into-holes bispecific antibody technology to the IgG4 isotype.

Despite the high sequence homology between human IgG1 and IgG4 isotypes (>90%), several key sequence differences (36) exist that may impact the functional expression in *E. coli* and the subsequent assembly of half-antibodies into a bispecific molecule *in vitro*. Importantly, in contrast to IgG1, the heavy-light interchain disulfide of IgG4 is formed by non-consecutive disulfides (Fig. 3). This non-consecutive disulfide linkage pattern is not commonly observed for *E. coli* proteins (37). In addition, the hinge region of IgG4 is destabilized by a Ser-228 residue, and the C_H3 dimer interface of IgG4 contains a destabilizing Arg-409 residue (38) (European Union numbering convention).

We designed several constructs to dissect the impact of the IgG4 Fc region sequence, the interchain disulfide pattern, and the C_H3 Arg-409 on the functional expression of the half-antibodies in *E. coli* and subsequent assembly to a bispecific molecule. In all cases, we introduced a stabilizing S228P mutation in the hinge region to attenuate Fab arm exchange after assembly (39). We first grafted the IgG4 Fc region with corresponding knob/hole mutations (6) (T366W, T366S, L368A, and Y407V) onto the IgG1 Fab in order to assess the impact of the IgG4 Fc region on functional expression of the half-antibody. For both antibodies, anti-IL-4 and anti-IL-13, this yielded similar amounts of disulfide-bonded material as the IgG1 isotype (Fig. 2, *c* and *d*), indicating that the differences between the isotypes in the Fc region do not impact functional half-antibody expression in *E. coli*. We next converted the entire constant region of the heavy chain to the IgG4 subclass. Although this resulted in a reduction in functionally expressed half-antibody, it demonstrated that *E. coli* is in principle capable of forming intramolecular disulfides in the constant region of the antibody from non-consecutive cysteines. Because position 409 is critical for the C_H3 stability (38) and the impact of Arg-409 for a downstream assembly process was uncertain at this stage, we also designed a construct with an R409K mutation, to recreate the C_H3 interface found in the IgG1 isotype. For both antibodies, this partially rescued the slight drop in functional expression of the IgG4 isotype (Fig. 2, *c* and *d*).

Assembly and Purification of Bispecific Antibodies—To compare the assembly of the different bispecific antibody constructs, we grew cultures expressing half-antibodies as IgG1, IgG4, and $IgG4_{R409K}$. After purification of the half-antibodies by Protein A chromatography, the hemimer pairs were mixed, and the intact bispecific antibody was formed by a redox chemistry step of the heterodimerized knob/hole pairs. Excess half-antibody was removed by anion and cation exchange chromatography steps. After the final chromatography step, the material was formulated at 45 g/liter in 0.2 M arginine succinate, pH 5.5, 0.02% polysorbate-20. To confirm that the assembled antibodies shifted from the half-antibody species to a stable intact antibody, we characterized them by size exclusion chromatography. All three constructs eluted with a retention time corresponding to an intact, 150-kDa antibody (Fig. 4*a*). Furthermore, no significant amounts of aggregated species (0.6/0.4/0.4% for IgG1/IgG4/$IgG4_{R409K}$) and only trace amounts of low molecular weight species (0.2/0/4.4% for IgG1/IgG4/$IgG4_{R409K}$) were detected, suggesting that both isotypes can be used to assemble antibodies of low aggregation propensity.

One of the critical steps during bispecific assembly is the formation of the hinge disulfides. Because size exclusion chromatography cannot resolve the oxidation state of the interchain disulfides, we subjected the antibodies to CE-SDS and found that all three formats formed hinge disulfides with similar efficiency. For IgG1, IgG4, and $IgG4_{R409K}$, 89.3, 91.4, and 86.7% of the material was observed in the fully oxidized conformation, respectively (Fig. 4*b*). We next reduced the samples and reanalyzed them by CE-SDS to determine the respective ratios of light to heavy chains (Fig. 4*c*). All three formats had a similar and expected distribution of light (31.3/31.4/30.9% for IgG1/

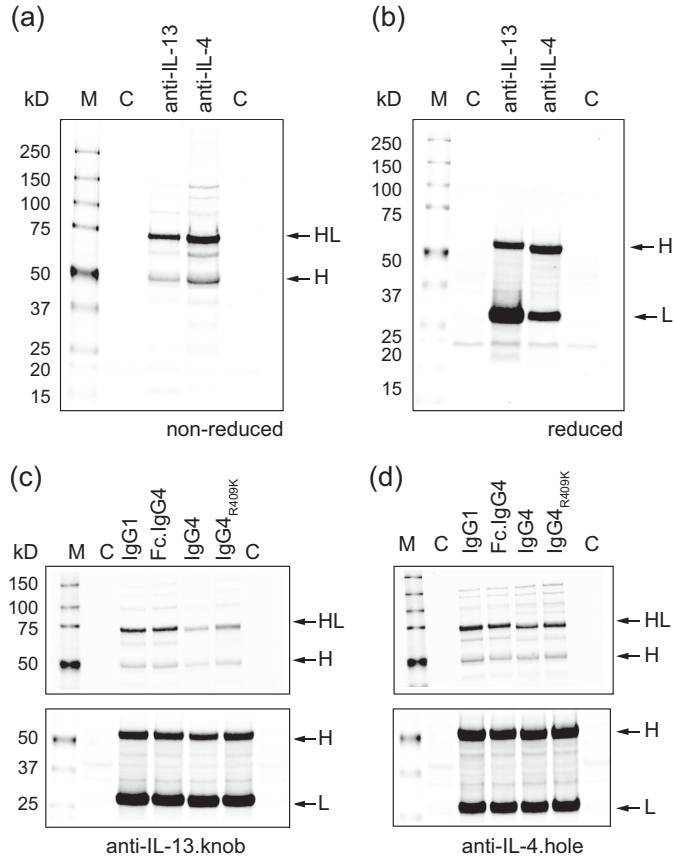

FIGURE 2. **Expression and Western blot analysis of knob and hole half-antibodies.** Shown is Western blot of non-reduced (*a*) and reduced (*b*) samples of anti-IL-13.knob and anti-IL-4.hole as IgG1-isotype in *E. coli*. The knob and hole mutations both result in a predominant half-antibody species (*HL*). Fragment designations are heavy chain (*H*) and light chain (*L*). *Lane M*, molecular weight standard; *lane C*, control (no antibody expression plasmid). An immunoblot compares the different isotypes and mutations for anti-IL-13.knob (*c*) and anti-IL-4.hole (*d*). The *top panel* under non-reduced conditions represents the assembled half-antibody. Although swapping only the Fc region from the IgG1 to IgG4 isotype (Fc.IgG4) has no impact on assembly, switching to a IgG4 isotype (IgG4, $IgG4_{R409K}$) reduced the overall amount of correctly folded half-antibody for both half-antibodies. The *bottom panel* under reducing conditions shows that similar amounts of heavy and light chain are synthesized for all variants, indicating that reduced amounts of intact half-antibody are caused by impaired folding and not synthesis.

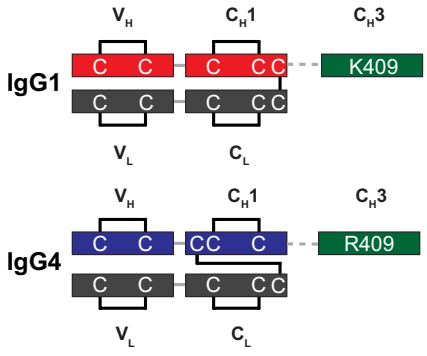

FIGURE 3. **Disulfide arrangement of human IgG1 and IgG4 isotypes.** IgG1 and IgG4 isotypes have different heavy-light interchain disulfide arrangements. In contrast to IgG1, the interchain disulfide of IgG4 is formed by the third cysteine in the heavy chain sequence. Although conserving the overall structure of the immunoglobulin fold, it results in a non-consecutive disulfide pattern in the C_H1 domain.

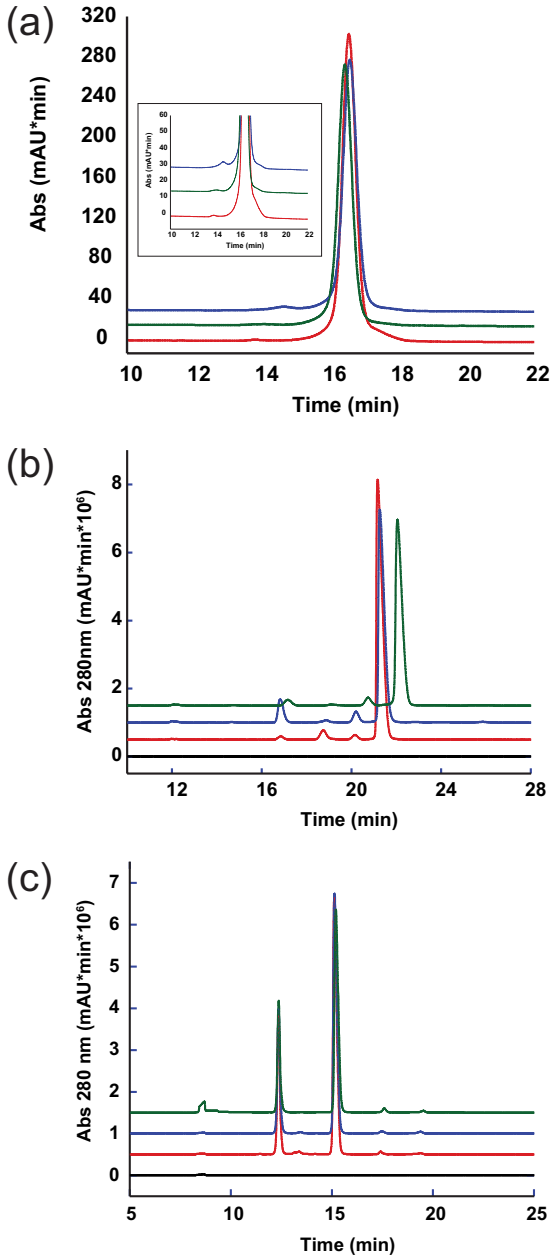

FIGURE 4. **Analytical characterization of the bispecific antibodies confirms successful assembly of the immunoglobulin.** *a*, size exclusion chromatography of the assembled material confirmed the intact 150-kDa species and low aggregate levels of the bispecific antibodies. The *inset* shows a *zoomed in view* of the same graph on the high molecular weight area. *b*, by non-reduced CE-SDS-PAGE, the successful formation of the hinge disulfides and the integrity of interchain disulfides were confirmed. The main peak area corresponds to an intact antibody with formed interchain disulfides. The few minor peak species are reflective of intact antibody lacking complete interchain disulfide to stabilize the heterodimer. *c*, reduced CE-SDS confirmed the presence of the expected distribution of light and heavy chains and demonstrated the purity of the material. Aside from the main peaks for intact light and heavy chain, only trace peaks were detected. For *all panels*, IgG1 (*green*), IgG4 (*red*), $IgG4_{R409K}$ (*blue*), and buffer only (*black*) are shown. *mAU*, milliabsorbance units.

IgG4/$IgG4_{R409K}$) and heavy chains (65.8/64.9/65.4% for IgG1/IgG4/$IgG4_{R409K}$), further confirming the existence of a natural antibody conformation.

To ensure that heterodimeric species were generated during the assembly process, we analyzed the final bispecific molecules

TABLE 1
Mass spectrometric analysis of non-reduced anti-IL-4/IL-13 bispecific antibodies

	Theoretical mass	Experimental mass
	Da	*Da*
Anti-IL-4/IL-13 IgG1 bispecific	145,298.4	145,304.5
Anti-IL-4 IgG1 homodimer	144,798.6	NO[a]
Anti-IL-13 IgG1 homodimer	145,798.3	NO
Anti-IL-4/IL-13 IgG4 bispecific	144,923.7	144,929.6
Anti-IL-4 IgG4 homodimer	144,423.9	NO
Anti-IL-13 IgG4 homodimer	145,423.5	NO
Anti-IL-4/IL-13 $IgG4_{R409K}$ bispecific	144,867.7	144,874.0
Anti-IL-4 $IgG4_{R409K}$ homodimer	144,367.8	NO
Anti-IL-13 $IgG4_{R409K}$ homodimer	145,367.5	NO

[a] NO, not observed.

TABLE 2
Mass spectrometric analysis of reduced anti-IL-4/IL-13 bispecific antibodies

	Theoretical mass	Experimental mass
	Da	*Da*
Anti-IL-4 LC[a] IgG1	23,522	23,521
Anti-IL-4 HC[b] IgG1	48,893	48,893
Anti-IL-13 LC IgG1	23,815	23,815
Anti-IL-13 HC IgG1	49,100	49,099
Anti-IL-4 LC IgG4	23,522	23,523
Anti-IL-4 HC IgG4	48,706	48,708
Anti-IL-13 LC IgG4	23,815	23,816
Anti-IL-13 HC IgG4	48,913	48,914
Anti-IL-4 LC $IgG4_{R409K}$	23,522	23,523
Anti-IL-4 HC $IgG4_{R409K}$	48,678	48,679
Anti-IL-13 LC $IgG4_{R409K}$	23,815	23,816
Anti-IL-13 HC $IgG4_{R409K}$	48,885	48,886

[a] LC, light chain.
[b] HC, heavy chain.

by mass spectrometry. The intact and reduced masses are summarized in Table 1 and Table 2. For all three bispecific antibodies, the experimental masses matched closely the theoretical masses, and we were not able to detect any masses corresponding to homodimeric species. A reverse phase HPLC assay further confirmed that the antibodies were bispecific, with no evidence of homodimeric antibodies (data not shown). Because we could not detect any significant differences in the assembly of Arg-409 and R409K IgG4 bispecific knobs-into-holes antibodies, all further studies utilized the wild type (Arg-409) IgG4 bispecific antibody format.

Biochemical Characterization of Bispecific Antibodies—We next characterized the IgG1 and IgG4 bispecific antibodies to assess whether their binding affinities to IL-4 and IL-13, as well as their ability to block the binding of IL-4 and IL-13 to their receptors, were comparable. The affinities of the IgG1 and IgG4 bispecific antibodies for IL-4 and IL-13 were measured by Biacore and were found to be comparable (Table 3) and similar to those of the parental antibodies, indicating that the ability to bind ligand is not impacted by the bispecific format or the isotype. In addition, similar to the parental anti-IL-4 and anti-IL-13 antibodies, each bispecific antibody fully inhibited the binding of IL-4 to IL-4Rα and did not inhibit binding of IL-13 to IL-13Rα1 or IL-13Rα2. These findings suggest that the binding epitope and monovalent affinity for each IL-13 and IL-4 arm was conserved across the bispecific antibodies.

TABLE 3
Binding kinetics of anti-IL-4/IL-13 bispecific antibodies

Isotype	Ligand	$K_{on}/10^4$	$k_{off}/10^{-4}$	K_d
		$M^{-1}\,s^{-1}$	s^{-1}	n_M
IgG1	IL-4	134.4 ± 49.8	0.848 ± 0.05	0.068 ± 0.020
IgG4	IL-4	287.00 ± 4.58	1.327 ± 0.058	0.046 ± 0.001
IgG1	IL-13	71.4 ± 4.0	0.170 ± 0.119	0.023 ± 0.015
IgG4	IL-13	53.73 ± 2.1	0.301 ± 0.109	0.056 ± 0.020

Neutralization of IL-4 and IL-13 Activity in an in Vitro Cellular Assay—The activity of both anti-IL-4/IL-13 IgG1 and anti-IL-4/IL-13 IgG4 bispecific antibodies was assessed in an *in vitro* cellular assay in which human IL-4 and IL-13 induce the proliferation of TF-1 cells. The ability of each bispecific antibody to block proliferation of TF-1 cells induced by human IL-4, human IL-13, and the human IL-13 isoform R130Q (data not shown) alone or in combination was evaluated (Fig. 5). Both anti-IL-4/IL-13 IgG1 and anti-IL-4/IL-13 IgG4 bispecific antibodies inhibited human IL-4-induced (IC_{50} = 0.06 μg/ml (IgG1) and 0.05 μg/ml (IgG4)), IL-13-induced (IC_{50} = 0.03 μg/ml (IgG1) and 0.03 μg/ml (IgG4)), and IL-4-/IL-13-induced (IC_{50} = 0.07 μg/ml (IgG1) and 0.05 μg/ml (IgG4)) proliferation of TF-1 cells in a dose-dependent manner, with no significant differences in the IC_{50} values for *in vitro* neutralization between the two different bispecific antibodies. In addition, each bispecific antibody neutralized IL-4-/IL-13-induced TF-1 cell proliferation with comparable potency as a combination of the two parental bivalent, monospecific antibodies (Fig. 5*d*), indicating that there is no loss of antibody potency in the bispecific antibody format.

Pharmacokinetic Studies in Cynomolgus Monkeys—We next assessed the *in vivo* pharmacokinetics of the IgG4 and IgG1 anti-IL-4/IL-13 bispecific antibodies following single intravenous or subcutaneous administration to cynomolgus monkeys. The serum concentration-time profiles of the anti-IL-4/IL-13 IgG4 and anti-IL-4/IL-13 IgG1 bispecific antibodies exhibited biphasic disposition with linear pharmacokinetics over the dose range tested (Fig. 6, *a* and *b*). The initial volume of the central compartment for both antibodies was similar to the serum volume, indicating limited distribution. Both antibodies had a relatively slow clearance and a long terminal half-life that was as expected for human IgG4 and IgG1 antibodies in cynomolgus monkeys (mean clearance = 5.79 – 6.70 ml/day/kg for anti-IL-4/IL-13 IgG4 and 3.59 – 4.09 ml/day/kg for anti-IL-4/IL-13 IgG1). Based on the area under the curve calculated for the 10 mg/kg dose groups, the subcutaneous bioavailability of the anti-IL-4/IL-13 IgG4 antibody was 95.1%. The presence of anti-therapeutic antibodies was detected in 50% of the anti-IL-4/IL-13 IgG4-dosed animals, including all three animals in the 100 mg/kg intravenous dose group, and appeared to be associated with the increased elimination of anti-IL-4/IL-13 IgG4 after day 14. There was a low incidence of anti-therapeutic antibodies detected in anti-IL-4/IL-13 IgG1-treated animals, which did not appear to affect the PK. Overall the pharmacokinetics of both anti-IL-4/IL-13 IgG4 and anti-IL-4/IL-13 IgG1 bispecific antibodies were similar and comparable with that of other humanized IgG1 and IgG4 monoclonal antibodies in cynomolgus monkeys.

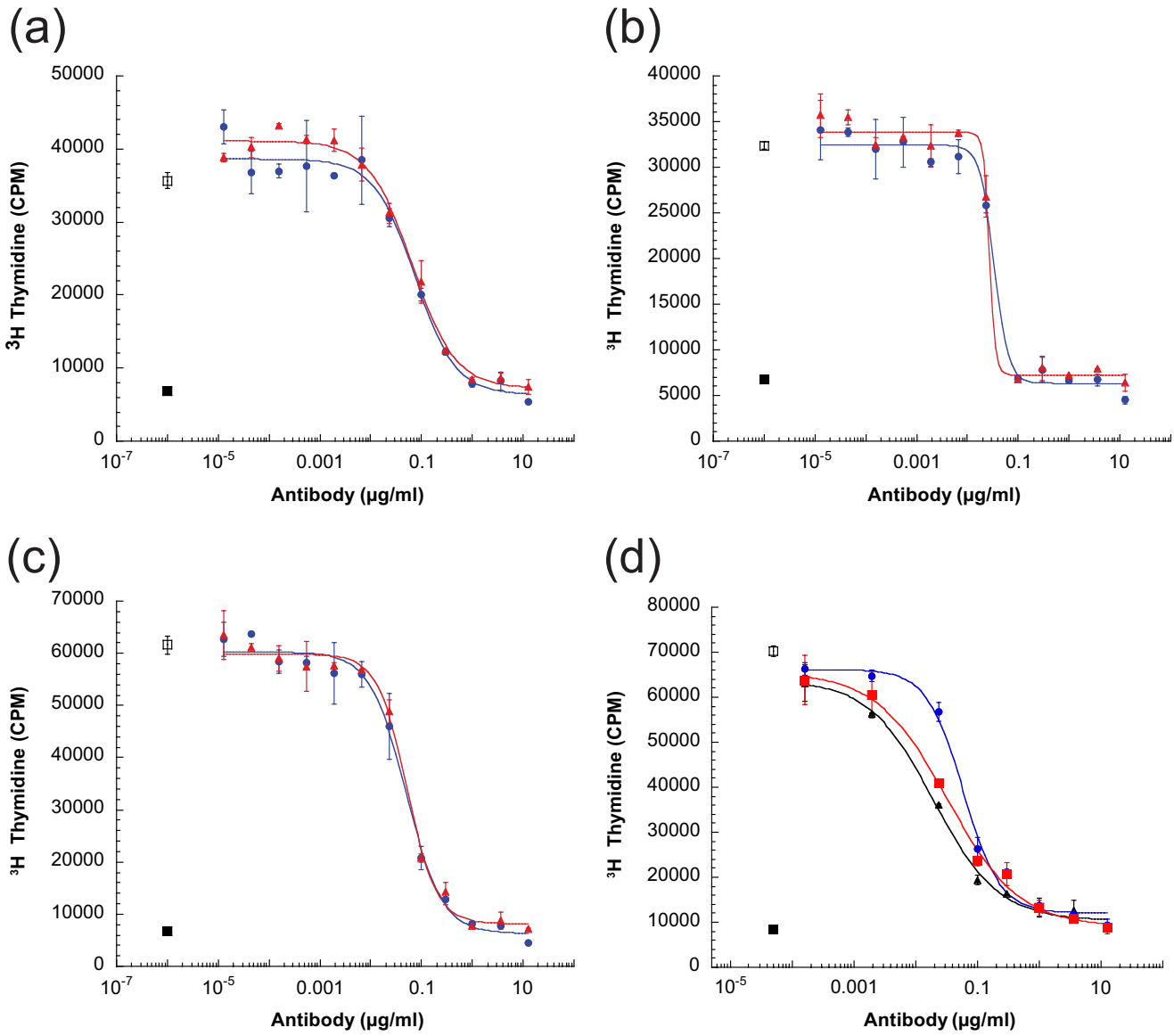

FIGURE 5. **Anti-IL-4/IL-13 bispecific antibodies potently inhibit human IL-4- and IL-13-induced cell proliferation.** The bispecific antibodies of IgG1 or IgG4 isotype inhibit cytokine-driven cell proliferation with similar dose-dependent response. TF-1 cells were mixed and incubated with preincubated cytokine/antibody mixtures of variable antibody concentration. The ability of antibody to block human cytokine-induced proliferation was assayed for IL-4-induced (*a*) or IL-13-induced (*b*) proliferation alone or in combination IL-4/IL-13 (*c*) and, for IL-4/IL-13-induced proliferation, compared with that of a combination of the parental bivalent, monospecific anti-IL-4, and anti-IL-13 antibodies (*d*). After incubation for 4 days, cell proliferation was measured by [^{3}H]thymidine incorporation. Cell-associated radioactivity was quantified by scintillation counting. Results are expressed as the mean of duplicate samples. Antibodies added in cytokine incubation were as follows: anti-IL-4/IL-13 IgG1-isotype (*blue bullet*), anti-IL-4/IL-13 IgG4-isotype (*red square*), a mixture of anti-IL-4 and anti-IL-13 (*black triangle*), no antibody added (*open square*), no cytokine and antibody added (*filled square*). *Error bars*, S.E.

Lung Partitioning in a Cynomolgus Monkey Asthma Model—Biodistribution of therapeutic antibodies to the lung is important in order to target local pathogenic IL-4 and IL-13 in asthmatics. Thus, we evaluated potential differences in the lung partitioning of IgG4 *versus* IgG1 anti-IL-4/IL-13-bispecific antibodies in a cynomolgus monkey model of asthma. In this asthma model, cynomolgus monkeys that were naturally sensitized to *A. suum* received an aerosol challenge of *A. suum* extract to elicit allergic inflammatory responses that mimic those of asthmatics exposed to allergens. We compared the serum concentrations to ELF concentrations of anti-IL-4/IL-13 IgG4 and anti-IL-4/IL-13 IgG1 antibodies following intravenous administration of 10 mg/kg on study days 1 and 8 and a lung challenge with *A. suum* extract on study day 9. IgG concentration values in the ELF were derived by correcting BAL fluid IgG concentration data for dilution inherent to the BAL fluid collection procedure as described (40). The serum to lung partitioning of anti-IL-4/IL-13 IgG4 and anti-IL-4/IL-13 IgG1 bispecific antibodies was comparable throughout the length of the study (Fig. 7). Prior to the allergen challenge, ELF concentrations for both antibodies were ~1–4% of IgG serum concentrations, indicating that only a small fraction of the systemic antibody reached the ELF. Inhalation challenge with *A. suum* on study day 9 appeared to result in increased lung partitioning for both antibodies. However, upon normalizing IgG concentrations to albumin concentrations in the ELF and comparing

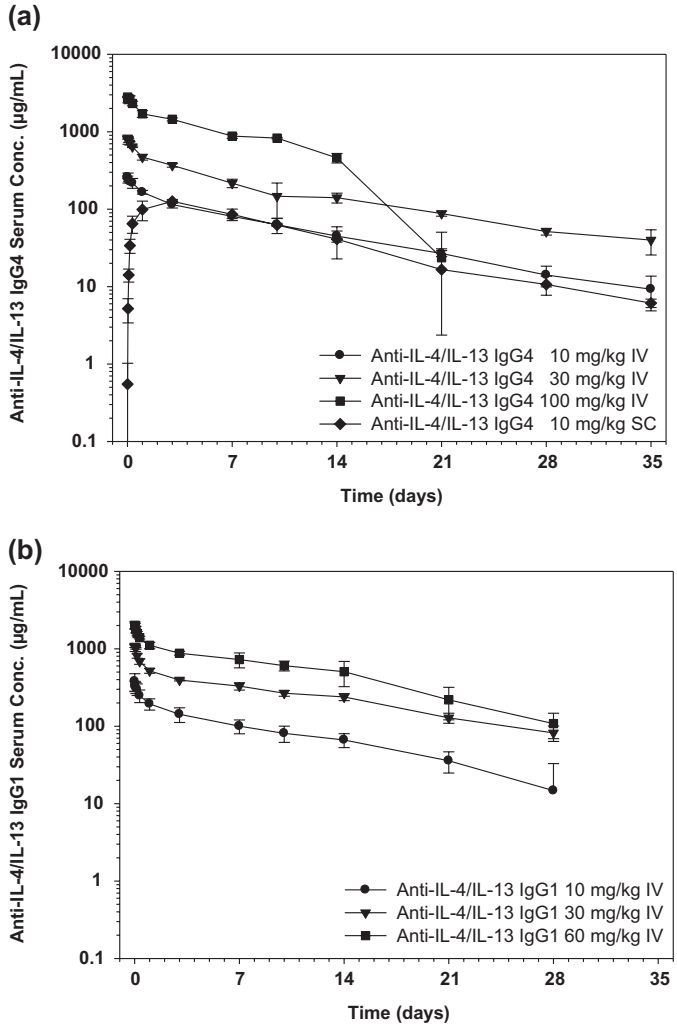

FIGURE 6. **Serum anti-IL-4/IL-13 concentrations following administration of a single intravenous or subcutaneous dose in cynomolgus monkeys.** We assessed the *in vivo* pharmacokinetics of the IgG4 and IgG1 anti-IL-4/IL-13 bispecific antibodies following single intravenous (*IV*) or subcutaneous (*SC*) administration to cynomolgus monkeys. The mean ± S.D. (n = 3/group) serum concentration-time profiles following single administration of anti-IL-4/IL-13 IgG4 at 10, 30, and 100 mg/kg intravenously and 10 mg/kg subcutaneously (*a*) or anti-IL-4/IL-13 IgG1 at 10, 30, and 60 mg/kg intravenously (*b*) to cynomolgus monkeys are shown. The limit of quantitation for the ELISA was 0.078 µg/ml. All data above the limit of quantitation were used, and all data below were excluded. S.D. (*error bars*) was not calculated when n was ≤2.

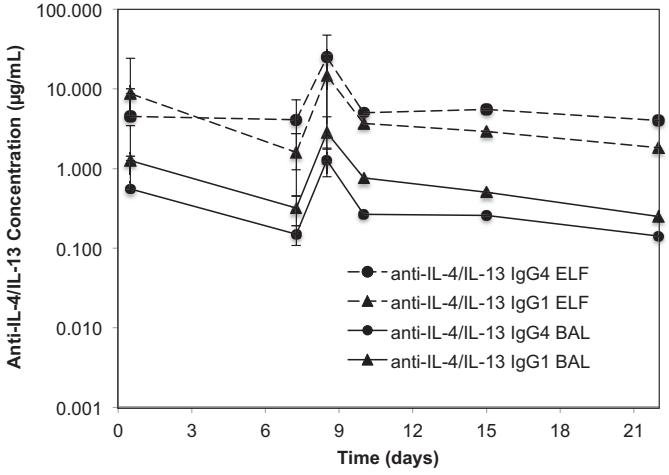

FIGURE 7. **BAL and ELF concentration values of anti-IL-4/IL-13 IgG4, and anti-IL-4/IL-13 IgG1 bispecific antibodies in cynomolgus monkeys.** We evaluated whether there were differences in the lung partitioning of IgG4 *versus* IgG1 anti-IL-4/IL-13 bispecific antibodies in a cynomolgus monkey model of asthma. In this asthma model, cynomolgus monkeys that are sensitized to *A. suum* are challenged with *A. suum* extract to elicit allergic inflammatory responses that mimic those of asthmatics exposed to allergens. Anti-IL-4/IL-13 concentration data in the ELF were derived by correcting BAL fluid concentration data for dilution inherent to the BAL fluid collection procedure. The mean ± S.D. (*error bars*) (n = 3–4/group) BAL fluid concentrations and ELF concentrations of anti-IL-4/IL-13 IgG4 and anti-IL-4/IL-13 IgG1 antibodies following intravenous administration of 10 mg/kg on study days 1 and 8 and a lung challenge with *A. suum* extract on study day 9 are shown. The limit of quantitation for the ELISA for anti-IL-4/IL-13 was 0.078 µg/ml. All data below the limit of quantitation were excluded; S.D. values were not calculated when n was ≤2.

these values with serum IgG concentrations, the data suggested that the increased ELF IgG concentrations following the respiratory challenge were due to nonspecific macromolecular vascular leakage induced by the challenge.

DISCUSSION

The development of new platforms for human bispecific antibodies may lead to more efficacious therapeutics for the treatment of human diseases. Current heterodimerization technologies to create full-length human IgG bispecific antibodies have only been reported for isotypes 1 and 2 (8–10, 12). Further extension of bispecific antibodies to other antibody isotypes as reported here will increase the diversity of bispecific antibody approaches for clinical applications.

Here we report the adaptation of the previously developed knobs-into-holes bispecific antibody platform to include human IgG4 antibodies and have applied this approach to generate bispecific antibodies against the cytokines IL-4 and IL-13. Given the overlapping and unique biologies of IL-4 and IL-13 as well as the activities of anti-IL-13 antibodies in the treatment of moderate to severe asthmatics, a bispecific antibody targeting both IL-4 and IL-13 may be an improved therapy over anti-IL-13 for the treatment of asthma. Our anti-IL-4/IL-13 bispecific antibody is an extension of the anti-IL-13 antibody lebrikizumab, which showed efficacy in a Phase II study in moderate to severe uncontrolled asthma. Because lebrikizumab is a human IgG4 antibody, we used the knobs-into-holes bispecific antibody platform to create a human IgG4 bispecific antibody in order to match the isotype of our anti-IL-4/IL-13 bispecific antibody to that of lebrikizumab. In addition to our anti-IL-4/IL-13 bispecific antibody, a tetravalent "dual variable domain" bispecific antibody that neutralizes IL-4 and IL-13 has been developed and is currently under clinical investigation (2). In contrast to the dual variable domain bispecific antibody format, our bispecific antibody preserves the natural surface architecture of an antibody and in addition allows the direct use of preexisting antibodies.

One of the key differences between human IgG1 and IgG4 isotypes is the C_H3 dimer interface, which affects the dimer stability. Differences are driven by position 409. Our results demonstrate that the knobs into holes mutations are compatible with Arg-409 in the C_H3 domain of IgG4, both in terms of expression as half-antibodies and assembly into a bispecific antibody. We could not detect any significant differences in the

assembly efficiency or in the quality of final antibody material between the two different isotypes.

Although the expression of human antibodies of various isotypes is well-established in mammalian cells, there have been fewer attempts to express different human antibody isotypes in *E. coli*, and the expression of full-length or half antibodies of human IgG4 isotype in *E. coli* has not been reported previously in the scientific literature. Here we demonstrate that human IgG4 hemimers can be successfully expressed in large quantities in *E. coli* cells and assembled into bispecific antibodies as readily as human IgG1 bispecific antibodies.

One of the hallmarks of the knobs-into-holes technology is the retention of the biophysical properties of the monovalent parental antibody in a final bispecific molecule. Both the IgG1 and IgG4 bispecific antibodies retained the target epitope and binding properties of the parental Fab, including high affinity to the IL-4 or IL-13 target cytokine, leading to high potency in *in vitro* cellular assays.

Pharmacokinetic studies in cynomolgus monkeys demonstrated slow clearance and similar terminal half-lives for both IgG1 and IgG4 bispecific antibodies. In addition, both IgG1 and IgG4 bispecific antibodies partitioned comparably from the serum to the lung at levels that may enable the complete neutralization of pathogenic IL-4 and IL-13 in the lung, which is important for the treatment of asthma. Although the IgG4 bispecific antibody appeared to have a higher rate of anti-therapeutic antibodies compared with the IgG1 bispecific antibody in cynomolgus monkeys, given the small number of animals used in our studies as well as the lack of a clear relationship between the immunogenicity of humanized antibodies in cynomolgus monkeys *versus* humans, we cannot make any conclusions about the relative immunogenicity of our anti-IL-4/IL-13 IgG4 and IgG1 bispecific antibodies in humans. It should be noted, however, that aside from the complementarity-determining regions of the antibody Fabs, our bispecific antibodies consist of fully human IgG1 and IgG4 sequences that should exhibit minimal immunogenicity in humans. Thus, the bispecific antibodies that we have generated are good candidates for clinical development for the treatment of asthma.

Antibodies of different human isotypes can have very different *in vitro* and *in vivo* properties, resulting from differences in binding to serum complement proteins and Fcγ receptors on immune effector cells (41). In particular, antibodies of human IgG1 isotype effectively activate the complement system and engage Fcγ receptors to trigger antibody-dependent cellular cytoxicity (ADCC), whereas antibodies of human IgG4 isotype do not activate the complement system and have reduced ADCC. Importantly, these properties of antibody effector function require antibody glycosylation that is generated during expression in mammalian cells. Antibodies produced in bacterial cells, such as *E. coli*, lack antibody effector function (33, 42) regardless of isotype, due to a lack of antibody glycosylation. Although the bispecific antibodies produced in this study are all produced in *E. coli* and therefore lack glycosylation and Fc effector function, efforts to produce these knobs-into-holes bispecific antibodies in mammalian cells are in progress. This approach provides further evidence that the knobs-into-holes bispecific antibody platform may include fully glycosylated human IgG1 and IgG4 antibody isotypes and may in turn provide a broad range of therapeutic bispecific antibodies with differing effector functions.

Acknowledgments—We thank members of the Antibody Engineering Department at Genentech for technical support and/or advice and stimulating discussions. In particular, we thank Anan Chuntharapai and Chae Reed for generating the anti-IL-4 hybridoma; Manda Wong for purification of cytokines; Vivian Lee for assay support; Arthur Huang, Noelle Lombana, and Daniel Yansura for technical help and advice regarding expression of antibodies in E. coli; Michelle W. Lee, Amy Lim, and Maricel Rodriguez for purification support; David Michels (Protein Analytical Chemistry Department) for support of CE development and analysis; Sally Fischer (Bioanalytical Sciences Department) for measuring the antibody levels; Leslie Khawli (Preclinical and Translational Pharmacokinetics and Pharmakodynamics Department) for guidance on the lung partitioning study design; and Carolina Chou (Nonclinical Operations Department) for managing the cyno studies.

REFERENCES

1. Kontermann, R. (2012) Dual targeting strategies with bispecific antibodies. *MAbs* **4,** 182–197
2. Dhimolea, E., and Reichert, J. M. (2012) World Bispecific Antibody Summit, September 27–28, 2011, Boston, MA. *MAbs* **4,** 4–13
3. Chelius, D., Ruf, P., Gruber, P., Plöscher, M., Liedtke, R., Gansberger, E., Hess, J., Wasiliu, M., and Lindhofer, H. (2010) Structural and functional characterization of the trifunctional antibody catumaxomab. *MAbs* **2,** 309–319
4. Dennis, M. S. (2002) Albumin binding as a general strategy for improving the pharmacokinetics of proteins. *J. Biol. Chem.* **277,** 35035–35043
5. Atwell, S., Ridgway, J. B., Wells, J. A., and Carter, P. (1997) Stable heterodimers from remodeling the domain interface of a homodimer using a phage display library. *J. Mol. Biol.* **270,** 26–35
6. Ridgway, J. B., Presta, L. G., and Carter, P. (1996) "Knobs-into-holes" engineering of antibody CH3 domains for heavy chain heterodimerization. *Protein Eng.* **9,** 617–621
7. Davis, J. H., Aperlo, C., Li, Y., Kurosawa, E., Lan, Y., Lo, K.-M., and Huston, J. S. (2010) SEEDbodies. Fusion proteins based on strand-exchange engineered domain (SEED) CH3 heterodimers in an Fc analogue platform for asymmetric binders or immunofusions and bispecific antibodies. *Protein Eng. Des. Sel.* **23,** 195–202
8. Gunasekaran, K., Pentony, M., Shen, M., Garrett, L., Forte, C., Woodward, A., Ng, S. B., Born, T., Retter, M., Manchulenko, K., Sweet, H., Foltz, I. N., Wittekind, M., and Yan, W. (2010) Enhancing antibody Fc heterodimer formation through electrostatic steering effects. Applications to bispecific molecules and monovalent IgG. *J. Biol. Chem.* **285,** 19637–19646
9. Strop, P., Ho, W.-H., Boustany, L. M., Abdiche, Y. N., Lindquist, K. C., Farias, S. E., Rickert, M., Appah, C. T., Pascua, E., Radcliffe, T., Sutton, J., Chaparro-Riggers, J., Chen, W., Casas, M. G., Chin, S. M., Wong, O. K., Liu, S.-H., Vergara, G., Shelton, D., Rajpal, A., and Pons, J. (2012) Generating bispecific human IgG1 and IgG2 antibodies from any antibody pair. *J. Mol. Biol.* **420,** 204–219
10. Labrijn, A. F., Meesters, J. I., de Goeij, B. E., van den Bremer, E. T., Neijssen, J., van Kampen, M. D., Strumane, K., Verploegen, S., Kundu, A., Gramer, M. J., van Berkel, P. H., van de Winkel, J. G., Schuurman, J., and Parren, P. W. (2013) Efficient generation of stable bispecific IgG1 by controlled Fab-arm exchange. *Proc. Natl. Acad. Sci. U.S.A.* **110,** 5145–5150
11. Merchant, A. M., Zhu, Z., Yuan, J. Q., Goddard, A., Adams, C. W., Presta, L. G., and Carter, P. (1998) An efficient route to human bispecific IgG. *Nat. Biotechnol.* **16,** 677–681
12. Jackman, J., Chen, Y., Huang, A., Moffat, B., Scheer, J. M., Leong, S. R., Lee, W. P., Zhang, J., Sharma, N., Lu, Y., Iyer, S., Shields, R. L., Chiang, N.,

Bauer, M. C., Wadley, D., Roose-Girma, M., Vandlen, R., Yansura, D. G., Wu, Y., and Wu, L. C. (2010) Development of a two-part strategy to identify a therapeutic human bispecific antibody that inhibits IgE receptor signaling. *J. Biol. Chem.* **285,** 20850–20859

13. Wranik, B. J., Christensen, E. L., Schaefer, G., Jackman, J. K., Vendel, A. C., and Eaton, D. (2012) LUZ-Y, a novel platform for the mammalian cell production of full-length IgG-bispecific antibodies. *J. Biol. Chem.* **287,** 43331–43339
14. Schaefer, W., Regula, J. T., Bähner, M., Schanzer, J., Croasdale, R., Dürr, H., Gassner, C., Georges, G., Kettenberger, H., Imhof-Jung, S., Schwaiger, M., Stubenrauch, K. G., Sustmann, C., Thomas, M., Scheuer, W., and Klein, C. (2011) Immunoglobulin domain crossover as a generic approach for the production of bispecific IgG antibodies. *Proc. Natl. Acad. Sci. U.S.A.* **108,** 11187–11192
15. Spiess, C., Merchant, M., Huang, A., Zheng, Z., Yang, N.-Y., Peng, J., Ellerman, D., Shatz, W., Reilly, D., Yansura, D. G., and Scheer, J. M. (2013) Bispecific antibodies with natural architecture produced by co-culture of bacteria expressing two distinct half-antibodies. *Nat. Biotechnol.* **31,** 753–758
16. Yu, Y. J., Zhang, Y., Kenrick, M., Hoyte, K., Luk, W., Lu, Y., Atwal, J., Elliott, J. M., Prabhu, S., Watts, R. J., and Dennis, M. S. (2011) Boosting brain uptake of a therapeutic antibody by reducing its affinity for a transcytosis target. *Sci. Transl. Med.* **3,** 84ra44
17. Hershey, G. K. (2003) IL-13 receptors and signaling pathways. An evolving web. *J. Allergy Clin. Immunol.* **111,** 677–690 ; quiz 691
18. Wynn, T. A. (2003) IL-13 effector functions. *Annu. Rev. Immunol.* **21,** 425–456
19. LaPorte, S. L., Juo, Z. S., Vaclavikova, J., Colf, L. A., Qi, X., Heller, N. M., Keegan, A. D., and Garcia, K. C. (2008) Molecular and structural basis of cytokine receptor pleiotropy in the interleukin-4/13 system. *Cell* **132,** 259–272
20. Mueller, T. D., Zhang, J.-L., Sebald, W., and Duschl, A. (2002) Structure, binding, and antagonists in the IL-4/IL-13 receptor system. *Biochim. Biophys. Acta* **1592,** 237–250
21. Nelms, K., Keegan, A. D., Zamorano, J., Ryan, J. J., and Paul, W. E. (1999) The IL-4 receptor. Signaling mechanisms and biologic functions. *Annu. Rev. Immunol.* **17,** 701–738
22. Wills-Karp, M. (2004) Interleukin-13 in asthma pathogenesis. *Immunol. Rev.* **202,** 175–190
23. Brightling, C. E., Saha, S., and Hollins, F. (2010) Interleukin-13. Prospects for new treatments. *Clin. Exp. Allergy* **40,** 42–49
24. Finkelman, F. D., Hogan, S. P., Hershey, G. K., Rothenberg, M. E., and Wills-Karp, M. (2010) Importance of cytokines in murine allergic airway disease and human asthma. *J. Immunol.* **184,** 1663–1674
25. Maes, T., Joos, G. F., and Brusselle, G. G. (2012) Targeting interleukin-4 in asthma. Lost in translation? *Am. J. Respir. Cell Mol. Biol.* **47,** 261–270
26. Steinke, J. W., and Borish, L. (2001) Th2 cytokines and asthma. Interleukin-4. Its role in the pathogenesis of asthma, and targeting it for asthma treatment with interleukin-4 receptor antagonists. *Respir. Res.* **2,** 66–70
27. Corren, J., Lemanske, R. F., Hanania, N. A., Korenblat, P. E., Parsey, M. V., Arron, J. R., Harris, J. M., Scheerens, H., Wu, L. C., Su, Z., Mosesova, S., Eisner, M. D., Bohen, S. P., and Matthews, J. G. (2011) Lebrikizumab treatment in adults with asthma. *N. Engl. J. Med.* **365,** 1088–1098
28. Gauvreau, G. M., Boulet, L.-P., Cockcroft, D. W., Fitzgerald, J. M., Carlsten, C., Davis, B. E., Deschesnes, F., Duong, M., Durn, B. L., Howie, K. J., Hui, L., Kasaian, M. T., Killian, K. J., Strinich, T. X., Watson, R. M., Y, N., Zhou, S., Raible, D., and O'Byrne, P. M. (2011) Effects of interleukin-13 blockade on allergen-induced airway responses in mild atopic asthma. *Am. J. Respir. Crit. Care Med.* **183,** 1007–1014
29. Piper, E., Brightling, C., Niven, R., Oh, C., Faggioni, R., Poon, K., She, D., Kell, C., May, R. D., Geba, G. P., and Molfino, N. A. (2013) A phase II placebo-controlled study of tralokinumab in moderate-to-severe asthma. *Eur. Respir. J.* **41,** 330–338
30. Ingram, J. L., and Kraft, M. (2012) IL-13 in asthma and allergic disease. Asthma phenotypes and targeted therapies. *J. Allergy Clin. Immunol.* **130,** 829–842; quiz 843–844
31. Webb, S. (2011) Attacks on asthma. *Nat. Biotechnol.* **29,** 860–863
32. Baker, K. N., Rendall, M. H., Patel, A., Boyd, P., Hoare, M., Freedman, R. B., and James, D. C. (2002) Rapid monitoring of recombinant protein products. A comparison of current technologies. *Trends Biotechnol.* **20,** 149–156
33. Simmons, L. C., Reilly, D., Klimowski, L., Raju, T. S., Meng, G., Sims, P., Hong, K., Shields, R. L., Damico, L. A., Rancatore, P., and Yansura, D. G. (2002) Expression of full-length immunoglobulins in *Escherichia coli*. Rapid and efficient production of aglycosylated antibodies. *J. Immunol. Methods* **263,** 133–147
34. Reilly, D. E., and Yansura, D. G. (2010) *Antibody Engineering* (Kontermann, R., and Dübel, S., eds), pp. 331–344, Springer, Berlin
35. Ultsch, M., Bevers, J., Nakamura, G., Vandlen, R., Kelley, R. F., Wu, L. C., and Eigenbrot, C. (2013) Structural basis of signaling blockade by anti-IL-13 antibody lebrikizumab. *J. Mol. Biol.* **425,** 1330–1339
36. Aalberse, R. C., and Schuurman, J. (2002) IgG4 breaking the rules. *Immunology* **105,** 9–19
37. Berkmen, M. (2005) The nonconsecutive disulfide bond of *Escherichia coli* phytase (AppA) renders it dependent on the protein-disulfide isomerase, DsbC. *J. Biol. Chem.* **280,** 11387–11394
38. Dall'Acqua, W., Simon, A. L., Mulkerrin, M. G., and Carter, P. (1998) Contribution of domain interface residues to the stability of antibody CH3 domain homodimers. *Biochemistry* **37,** 9266–9273
39. Stubenrauch, K., Wessels, U., Regula, J. T., Kettenberger, H., Schleypen, J., and Kohnert, U. (2010) Impact of molecular processing in the hinge region of therapeutic IgG4 antibodies on disposition profiles in cynomolgus monkeys. *Drug Metab. Dispos.* **38,** 84–91
40. Rennard, S. I., Basset, G., Lecossier, D., O'Donnell, K. M., Pinkston, P., Martin, P. G., and Crystal, R. G. (1986) Estimation of volume of epithelial lining fluid recovered by lavage using urea as marker of dilution. *J. Appl. Physiol.* **60,** 532–538
41. Nirula, A., Glaser, S. M., Kalled, S. L., and Taylor, F. R. (2011) What is IgG4? A review of the biology of a unique immunoglobulin subtype. *Curr. Opin. Rheumatol.* **23,** 119–124
42. Jung, S. T., Kang, T. H., Kelton, W., and Georgiou, G. (2011) Bypassing glycosylation. Engineering aglycosylated full-length IgG antibodies for human therapy. *Curr. Opin. Biotechnol.* **22,** 858–867